01

Possibilities of X-ray spectral diagnostics of the collision region of laser-plasma flows with astrophysical similarity

© S.N. Ryazantsev[1], M.P. Filimonchuk[1,2], R.K. Kulikov[1,3], I.Yu. Skobelev[1,3], S.S. Makarov[1]

[1] Joint Institute for High Temperatures of the Russian Academy of Sciences (JIHT RAS), Moscow, Russia
[2] Moscow State University, Faculty of Physics, Moscow, Russia
[3] National Research Nuclear University „MEPhI", Moscow, Russia

e-mail: ryazantsev@ihed.ras.ru

Received October 08, 2024
Revised March 05, 2024
Accepted March 05, 2025

It is shown that spatially resolved registration of spectral lines of the resonance series of He-like ions can be used both for diagnostics of plasma parameters in the collision region of plasma flows generated by heating solid targets with laser radiation and for the determination of the spatial position of this region. The presented calculation results obtained in the quasi-stationary approximation for aluminum plasma can be used to determine the electron density and temperature in the range of $10^{18} - 10^{21}$ cm^{-3}. Using a hydrodynamic code, simple estimates of the increase in plasma density in the region of collision of laser-plasma jets are made.

Keywords: laboratory astrophysics, laser plasma, X-ray spectroscopy, plasma flows.

DOI: 10.61011/EOS.2025.04.61404.7149-24

Introduction

The use of colliding plasma flows (CPFs), including laser ones, is a current trend in laser-plasma experiments. This is attributable to the fact that data on the dependences of collision process parameters on experimental conditions may find various uses in applied and fundamental research. For example, the application of CPFs as a source of soft X-ray and ultraviolet radiation was discussed in [1]. The issue of reduction of efficiency of experimental thermonuclear reactors is associated with CPFs near the vacuum chamber walls [2,3]. A deeper understanding of processes proceeding in the region of plasma flow collisions should contribute to an improvement in the accuracy of laser-induced spark emission spectrometry [4,5]. Naturally, experiments with colliding flows may be used in fundamental research into the origin of hydrodynamic plasma instabilities, the propagation of shock waves in low-temperature plasma, and other hydrodynamic phenomena. CPFs are of particular interest in the context of experiments on modeling of astrophysical jets [6] with laser-induced plasma flows. This modeling is based on the principles of similarity of magnetohydrodynamic systems outlined in [7].

The life cycle of a jet may be divided into two stages: formation and propagation. Each of them poses its own questions to researchers. Some of them are associated with one of the key features of jets, namely a high degree of collimation (i.e., the ratio between length L of a jet and its diameter D, which may reach $L/D \gg 10$). The current understanding is that a jet is collimated directly at the formation stage in the immediate vicinity of its origin object (e.g., a forming star). The theory behind the mechanism of this process is still under development, although there is a consensus that it is driven by magnetic fields. For example, it was demonstrated in a series of studies [8–10] that laser plasma is drawn into a jet with ratio $L/D \geq 10$ under the influence of a uniform field with its lines of force being perpendicular to the surface of the target.

The issue of maintaining a high degree of collimation at significant distances from the source of a jet, which may extend over tens and even hundreds of parsecs [6,11], is no less important. This effect may be associated with the interaction of jet matter with interstellar gas [12]. To test this theory in a laboratory experiment, one needs to establish such conditions under which the influence of the mechanism collimating a jet at the stage of its formation is suppressed at the propagation stage. Basically, there are two different ways to achieve this: one should either ensure that the collimated flow exits the region of existence of an external magnetic field [13] or should not use it for collimation at all. The latter scenario leads to the idea of colliding plasma flows. For example, it was demonstrated experimentally in [11,14] that a collision of two laser plasma flows propagating at an angle to each other results in the formation of a collimated jet.

Radiography [15,16] (phase-contrast one included [17,18]), laser interferometry [19,20], and spectrometry, including X-ray techniques, are commonly used to identify plasma parameters in the region of such a collision. The present study is focused on an approach to such diagnostics based on the analysis of line emission spectra that undergo drastic changes in relative intensities of lines of the resonance series of multicharged He-like ions in the collision region. Detailed calculations are performed for an aluminum target.

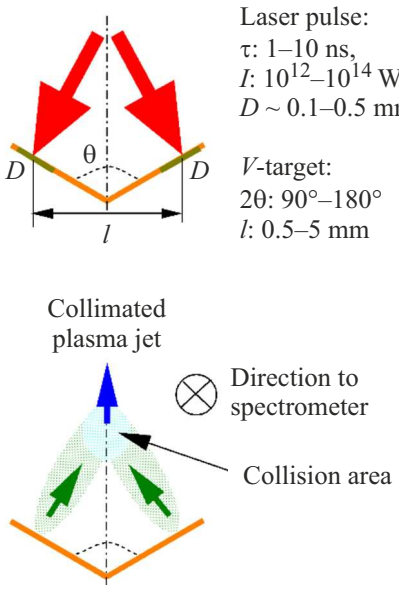

Figure 1. Diagram of the experiment on collision of plasma flows produced by irradiating a *V*-shaped target. Two flat targets with a thickness of several tens of micrometers are positioned at angle θ (the cases of $2\theta = 180°$ and $2\theta = 90°$ are examined here) to the central axis. These two foils are exposed to laser radiation simultaneously. Plasma plumes produced as a result of irradiation collide and form a collimated flow that propagates along the axis of symmetry of the target.

Emission spectra of plasma in the region of collision of laser-plasma flows

Let us consider the collision of two plasma flows formed by heating solid aluminum targets with high-intensity laser pulses of a comparatively long (nanosecond or subnanosecond) duration (Fig. 1). It should be stressed that such laser irradiation parameters are typical of current experiments in laboratory astrophysics.

The interaction of each laser pulse with a flat solid target leads to the formation of a laser-plasma plume with high temperature (hundreds of electron volts) and density (on the order of the critical one corresponding to the laser wavelength used) values near the target that decrease with distance from it. The state of plasma is ionizing (the degree of ionization is lower than the steady-state value at a given temperature) near the target, but becomes recombining (the degree of ionization is higher than the steady-state value at the local temperature) as one moves away from it.

Plasma plumes collide at a certain distance from the target. The plasma density and the electron temperature should naturally increase sharply in this region, affecting the emission spectrum of plasma. If the recorded emission spectrum is spatially resolved, the variations of its shape and intensity with spatial coordinate provide an opportunity to identify both the position of the collision region and the parameters of plasma in it. To do this, one needs to perform the corresponding calculations of radiation-collisional kinetics that determine the type of emission spectra. This problem has traditionally been solved for laser plasma in either steady or ionizing states that are characteristic of plasma regions close to the target surface [21]. In the examined case, the state of plasma in each of the plasma flows ahead of the collision region and in the collision region itself is recombining. This implies that kinetic calculations should be carried out within a quasi-stationary model [22]. The *iPRAX* [23] radiation-collisional code was used for this purpose in the present study.

It should be emphasized that the diagnostic capabilities of X-ray spectral methods applied to the region of jet collisions naturally depend on the intensity of variation of the plasma parameters in this region. The density and temperature jumps in the collision region may be estimated via hydrodynamic modeling. This was done here using modular code *PLUTO* [24].

Estimation of the density difference in the region of collision of plasma flows

The *HD* module from the standard set was the one actually used for modeling. The following system of equations was solved numerically in it in a two-dimensional Cartesian coordinate system:

$$\frac{\partial \rho}{\partial t} + \nabla(\rho v) = 0,$$

$$\frac{\partial m_x}{\partial t} + \nabla(m_x v) + \frac{\partial p_t}{\partial x} = 0,$$

$$\frac{\partial m_y}{\partial t} + \nabla(m_y v) + \frac{\partial p_t}{\partial y} = 0,$$

$$\frac{\partial}{\partial t} E_t + \nabla[(E_t + p_t)v] = 0,$$

where ρ is the mass density, (m_x, m_y) are the components of volume momentum density vector $m = \rho v$, v is the flow velocity, p_t is the pressure in the medium, and E_t is the total energy density defined as

$$E_t = \rho_e + \frac{m^2}{2\rho}.$$

Here, ρ_e is the internal energy density. The freeware *PLUTO* code distribution package is intended for modeling an ideal gas; i.e., the thermal equation of state is $p_t = n(\rho)k_B T$, where n is the particle concentration, k_B is the Boltzmann constant, and T is temperature, while the caloric equation is $\rho_e = \frac{p_t}{\gamma - 1}$, where $\gamma = 5/3$ is the adiabatic index. The second-order Lax–Friedrichs ($tvdlf$) and Runge–Kutta ($RK2$) schemes were used to solve the system (to determine the time evolution). The code operates on dimensionless quantities defined as q_{CGS}/q, where q_{CGS} is the CGS value of a quantity and q is the scale factor for this quantity. The scale factors for density, length, and velocity must be specified by the user. The

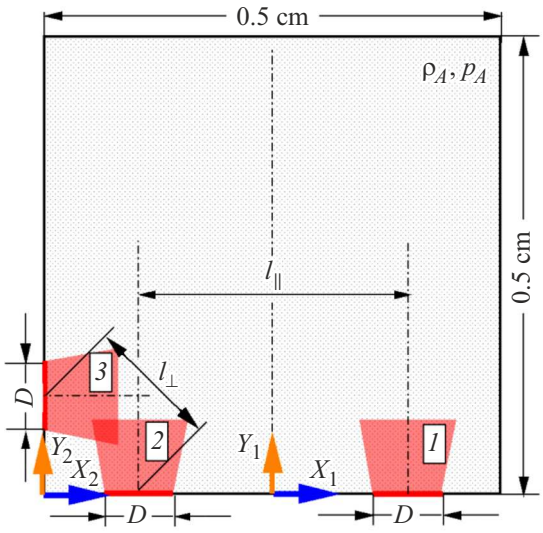

Figure 2. General diagram of the calculation field for hydrodynamic modeling.

factors for other quantities are recalculated based on the entered values. The following scale factors were used for calculations: $\rho = 1\,\text{g/cm}^3$ for density, $l = 1\,\text{cm}$ for length, and $v = 10^5\,\text{cm/s}$ for velocity.

The general diagram of the calculation field is shown in Fig. 2. The calculations were carried out on a uniform (cell size $d = 0.0025\,\text{cm}$) grid $0.5 \times 0.5\,\text{cm}$ (200×200) in size. To form a plasma inflow into the simulation field, the following fixed boundary conditions for density, pressure, and velocity were set in sections $D = 0.35\,\text{mm}$ with their centers separated spatially by $l_\parallel(l_\perp) = \{0.08\,\text{cm}, 0.1\,\text{cm}\}$: $\rho = 4 \cdot 10^{-6}\,\text{g/cm}^3$, $p_t = 10^7\,\text{dyne/cm}^2$ (1 MPa). The method for specifying velocity components (v_x, v_y) within regions D varied depending on the task. In the case of parallel expansion in coordinate system (X_1, Y_1),

$$v_x(x) = v_0 \sin[2\alpha(x \pm dx)/D],$$

$$v_y(x) = v_0 \cos[2\alpha(x \pm dx)/D],$$

where $d_x = l_\parallel/2$ and „–“ and „+“ are set for regions „1“ and „2,“ respectively. In the case of a single flow, $d_x = 0$. Region „2“ with perpendicular expansion in coordinate system (X_2, Y_2) has

$$v_x(x) = v_0 \sin[2\alpha(x - dx)/D],$$

$$v_y(x) = v_0 \cos[2\alpha(x - dx)/D],$$

while region „3“ has

$$v_x(y) = v_0 \cos[2\alpha(y - dx)/D],$$

$$v_y(y) = v_0 \sin[2\alpha(y - dx)/D],$$

where $d_x = l_\perp/\sqrt{2}$. The opening of the plasma expansion cone is $2\alpha = 80°$ in all cases, and $v_0 = 2 \cdot 10^7\,\text{cm/s}$ is the absolute value of the plasma flow velocity vector. Its direction varies from 0 to α in proportion to the value of coordinate x relative to the flow axis, $x \in [0, D/2]$. The indicated values of physical quantities are characteristic of flows of laboratory laser plasma generated by nanosecond laser pulses with an intensity of $\sim 1E13\,\text{W/cm}^2$ [13]. The value of $p_A = 1.3\,\text{dyne/cm}^2$ $(10^{-5}\,\text{Torr})$, which is typical for laser-plasma experiments and corresponds to density $\rho_A \approx 5.3 \cdot 10^{-11}\,\text{g/cm}^3$ at temperature $T = 300\,\text{K}$, was set as the residual medium pressure. Open boundary conditions were set along the entire perimeter of the simulation field (except for regions D); i.e., condition $\frac{\partial q}{\partial n} = 0$, where n is the coordinate axis perpendicular to a given boundary, was satisfied for all quantities q.

The simulated concentration maps corresponding to time point $t = 28\,\text{ns}$ and three different inflow cases are shown in Figs. 3, *a*–*c*. For ease of comparison, the calibration scale is the same in all panels. The time point was chosen so as to enable direct comparison of simulated data with the experimental free-expansion interferometer patterns presented in Fig. 2, *a* in [13]. Both Fig. 3, *b* and Fig. 3, *c* show clearly the regions of increased density forming when flows collide. However, these regions have significantly different morphologies. In the case of perpendicular flows, the forming single plasma flow has an expansion angle that is considerably smaller $(2\beta \sim 34°)$ than the original ones; i.e., plasma flows are actually collimated, which is confirmed by experimental data [11]. The pattern found in the case of coaxial expansion is different. A low-density „cavity“ is seen in the center of the collision region. However, it follows from Fig. 3, *d* that the density in the „cavity“ exceed the values for free expansion at distances up to distances 0.5 cm. The maximum excess in parallel expansion is achieved at a distance of $\sim 0.05\,\text{cm}$, where $k_\parallel = N_\parallel/N_f = 2.3$. In the case of perpendicular expansion, the maximum values are $k_\perp(0.044) = 5.3$ and $k_\perp(0.039) = 5.9$ at $l = 1\,\text{mm}$ and $l = 0.8\,\text{mm}$, respectively.

Thus, at typical parameters of experiments on laboratory modeling of astrophysical jets with irradiation of solid targets with laser pulses ($\tau_{las} \sim 1 - 10\,\text{ns}$, $10^{12} \le I_{las} \le 10^{14}\,\text{W/cm}^2$, $D \sim 0.01 - 0.05\,\text{cm}$), a ~ 6-fold jump in plasma density is to be expected in the region of collision of the resulting plasma flows. Assuming the process is adiabatic, this may also lead to a certain (less than 2-fold) increase in electron temperature. However, it cannot alter the nature of ionization state of plasma, which remains recombining in the collision region.

Radiation-collisional kinetics calculations

One first needs to determine which spectral lines are the most promising for diagnostics of the plasma object under consideration. Since its ionization state is expected to be recombining and the electron temperature is quite low, the intensities of dielectronic satellites of resonance lines commonly used for diagnostics are too low to be applicable in this case. Suitable lines are those induced

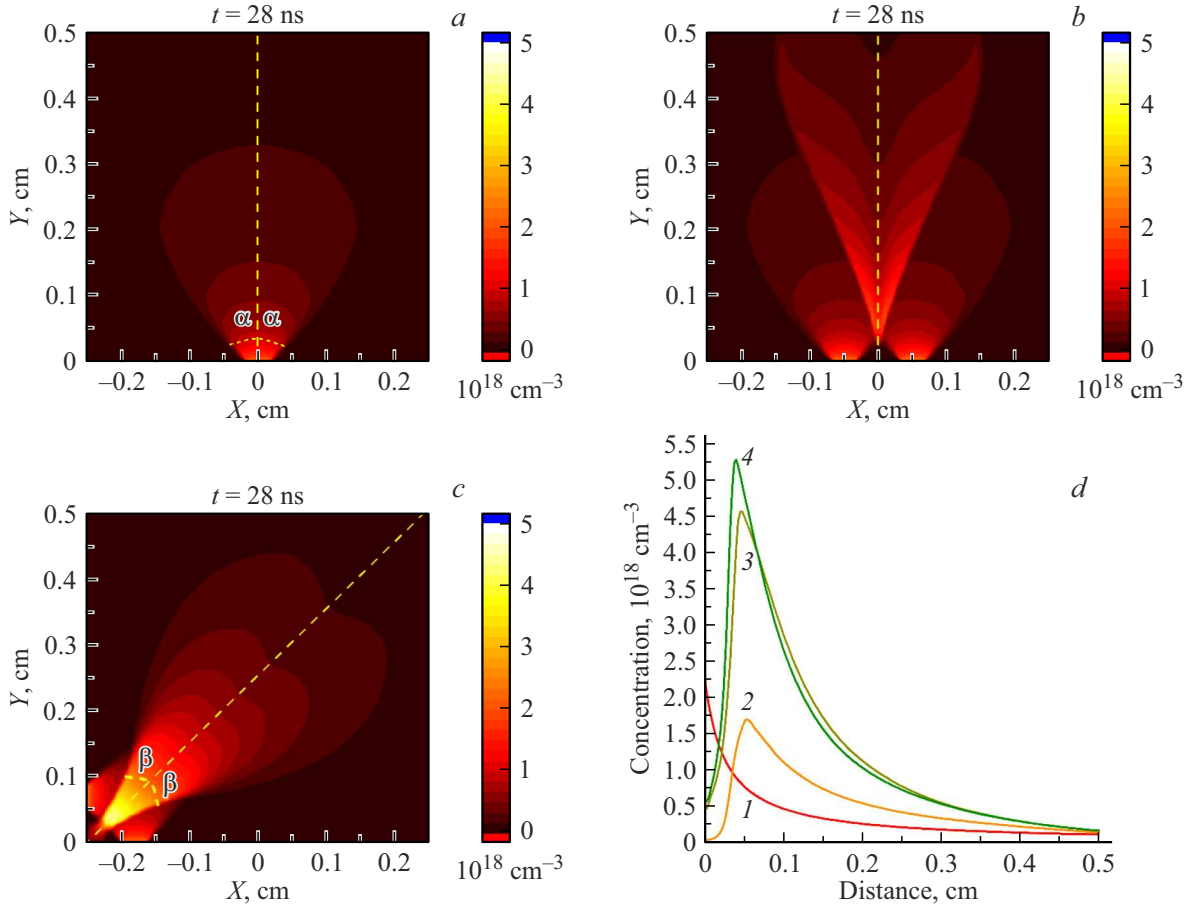

Figure 3. Concentration maps (ions per cm^{-3}) at time point $t = 28$ ns predicted by hydrodynamic modeling for (*a*) a single flow and two flows identical to (*a*) with (*b*) parallel ($l_{\parallel} = 1$ mm) and (*c*) perpendicular ($l_{\perp} = 0.1$ cm) expansion axes. (*d*) Profiles of variation of concentration *1*, *2*, and *3* along the yellow dashed lines in panels (*a*), (*b*), and (*c*), respectively. Profile *4* is similar to *3*, but with $l_{\perp} = 0.08$ cm.

by transitions between excited states of ions with the main K shell (H- and He-like) or between excited and ground states. In the present study, we examine only the latter lines, namely the resonance series of a He-like ion. They were chosen for the reliability and accuracy of detection, which is attributable to their relatively simple structure and the availability of well-established X-ray spectral measurement instruments (e.g., spectrometers based on spherically curved crystals [25]). It should be noted that the wavelengths of transitions between excited levels for ions with $Z \sim Z_{Al}$ should lie in the ultraviolet region, and the spectrometers discussed in [25] are inapplicable to their detection.

Kinetic calculations were performed for aluminum ions using the *iPRAX* radiation-collisional code. The atomic model included states of fully ionized aluminum, states of H-like Al XIII with principal quantum numbers up to 9, states of He-like Al XII with principal quantum numbers up to 7, states of Li-like Al X with principal quantum numbers up to 7, and the ground state of a Be-like ion. A total of 860 states were factored in. The calculation results are shown in Fig. 4.

Figure 4, *a* shows the dependences of the intensity ratio of intercombination and resonance Al XII He_{α} lines on plasma density at different temperatures. It is evident that this ratio is virtually independent of plasma temperature, but is sensitive to its density within a wide range of $10^{12} - 10^{23}$ cm^{-3}. This makes it convenient for diagnostics of this plasma parameter. Figure 4, *b* presents similar dependences for the intensity ratio of lines He_{β} and He_{α}. It can be seen that their range of density sensitivity is significantly narrower and starts from $\sim 10^{18}$ cm^{-3}. Line He_{β} is a more convenient comparison object for the spectral lines induced by transitions from levels with $n > 3$. The dependences for the $He_{\gamma}(n = 4)/He_{\beta}$ and $He_{\delta}(n = 5)/He_{\beta}$ ratios are shown as an example in Figs. 4, *c, d*. With the exception of $He_{int.}/He_{\alpha}$, all the presented ratios depend both on density and on electron temperature. Thus, one may determine the values of both plasma parameters using any two of these ratios.

The presented dependences provide an opportunity to estimate changes in the plasma emission spectrum in the region of collision of plasma flows. For example, the He_{γ}/He_{β} intensity ratio increases from 0.8 to 1.4 as the

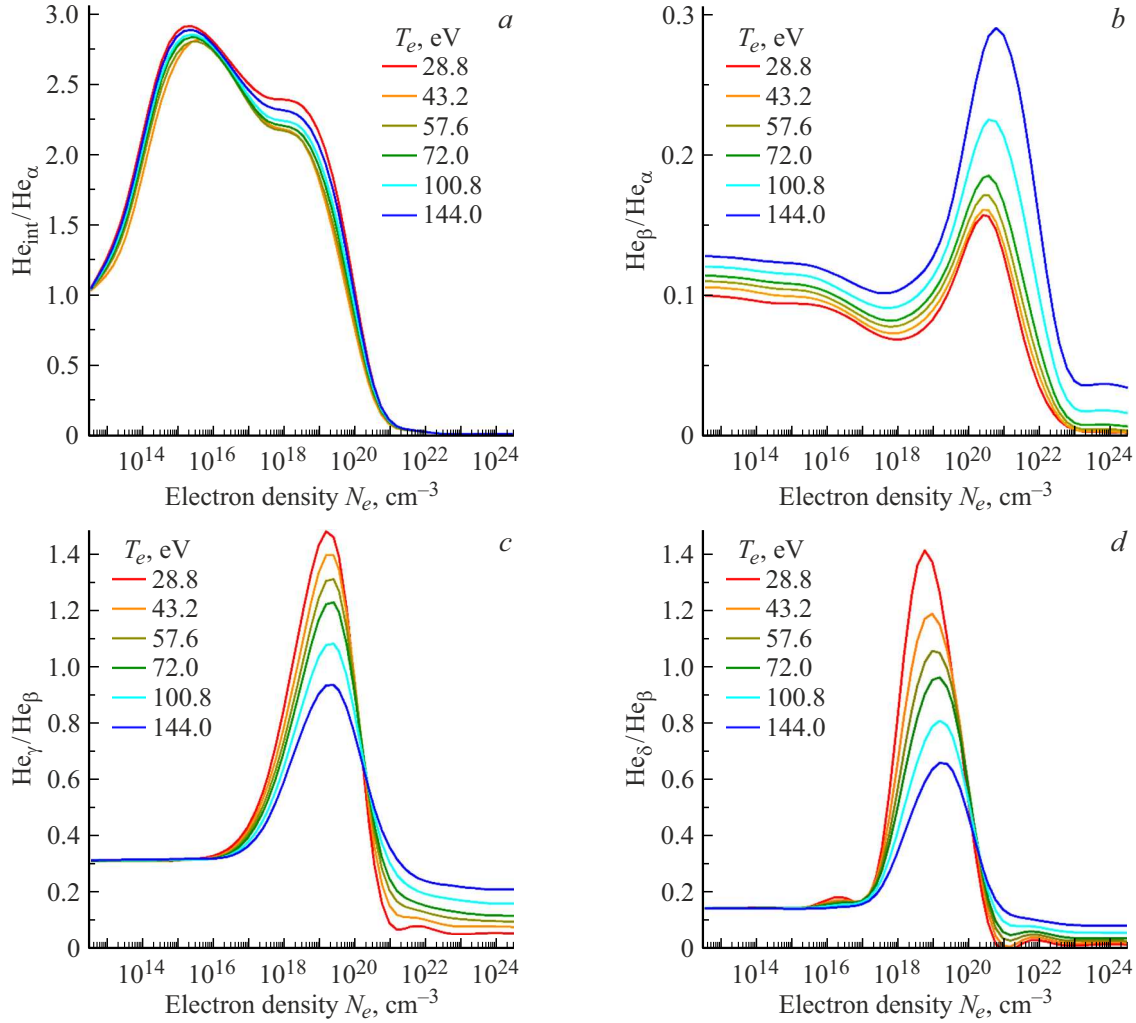

Figure 4. Dependences of the ratio of intensities of spectral lines emitted by recombining plasma during transitions in a He-like Al ion on electron density N_e at different values of electron temperature T_e. All spectral lines correspond to the transition to ground state $^1S_0\ 1s^2$ from an excited state: (*a*) $1s2p\,^1P_1$ for He_α, $1s2p\,^3P_1$ for He_{int}; (*b*) $1s3p\,^1P_1$ for He_β; (*c*) $1s4p\,^1P_1$ for He_γ; and (*d*) $1s5p\,^1P_1$ for He_δ.

density changes by a factor of 6 (e.g., from 10^{18} to $6 \cdot 10^{18}$ cm^{-3}). This change is sufficient for its reliable experimental detection. Therefore, the proposed X-ray spectral diagnostic technique should allow one to distinguish with certainty between the regions of free expansion of plasma jets and the regions of their collision.

Conclusion

It follows from the presented figures that the considered relative intensities of spectral lines of the Al XII ion are sensitive to the electron density of plasma within the range of $10^{18} - 10^{21}$ cm^{-3}. If a region of collision of jets with lower or higher densities needs to be examined, one may used targets of lighter or heavier ions, respectively.

Dependences similar to those presented in Fig. 4 (except for panel (*a*)) may be obtained for other He-like ions without performing additional calculations. Since the probabilities of allowed atomic transitions in He-like ions at $Z \sim 10$ should scale along the isoelectronic sequence according to the same laws as for H-like ions, the boundaries of ranges of sensitivity of the relative intensities to temperature and plasma density should shift in proportion to $\sim Z^2$ and $\sim Z^7$ [26].

The rough estimates made above with the *PLUTO* code demonstrate that an almost order-of-magnitude jump in density is to be expected in the region of collision of plasma flows. According to Fig. 4, this corresponds to at least a several-fold change in relative intensities (that is, if the density values fall within the optimum diagnostics range). In actual fact, even much smaller density jumps (e.g., 2-fold) will allow one to distinguish easily the spectra emitted by the collision region from the spectra emitted in free expansion of plasma.

Thus, observation of the resonance series lines of He-like ions may be used for diagnostics of parameters of recombining laser-plasma flows within fairly wide ranges of their temperatures and densities. The limitations of this

technique lie in the assumption regarding the recombining nature of plasma and the sufficiently small optical thickness in the spectral lines under consideration. The recombining nature of plasma is established automatically as a jet propagates over a sufficient distance from the region of its generation. This implies that the region of collision of jets should also lie far from the target, which may be achieved by setting a sufficiently large distance between the positions of focal spots of two laser beams. Within the range of electron densities of interest to us ($10^{16} - 10^{19}\,\mathrm{cm}^{-3}$), which corresponds to the results of hydrodynamic modeling, and at a temperature of 144 eV, the optical thickness varies within the interval of $10^{-2} - 10$ with a characteristic plasma size of 1 mm. However, according to [21], self-absorption effects do not affect the resonance line intensity if condition $A/(r+1) > N_e < \sigma v >$ (A is the probability of radiative decay of state $^1P_1$, $N_e < \sigma v >$ is the overall probability of collisional decay of the resonance level, and r is the optical thickness of plasma) is satisfied in the Biberman–Holstein approximation for self-absorption that is used in the *iPRAX* code. Note that this refers to the total spectral line intensity (i.e., the total energy of all photons emitted in a given radiative transition) and not to the spectral intensity at the line center. Specifically, it follows from calculated data that this condition is satisfied at $r < 700$ for plasma at a temperature of 144 eV and a density of $10^{19}\,\mathrm{cm}^{-3}$.

It should be noted that the use of the Biberman–Holstein approximation implies a complete frequency redistribution in photon scattering, and coherent scattering may be neglected. This imposes another restriction on the optical thickness of plasma, which is derived from the condition that the self-absorption line width should lie within the Doppler core. Since Doppler core width Ω_D may be estimated as $\Omega_D > \Delta\omega_D(\ln(2\pi^{3/2}\Delta\omega_D/\gamma))^{1/2}$ ($\Delta\omega_D$ and γ are the Doppler and natural line widths, respectively) [27], this condition actually comes down to restriction $r \leq (\Delta\omega_D/\gamma)$. The natural width of the broadest optical line He_α of the examined Al XII ion is $\gamma \sim 2.8 \cdot 10^{13}\,\mathrm{s}^{-1}$, and $\Delta\omega_D \sim 2.8 \cdot 10^{14}\,\mathrm{s}^{-1}$ at the considered plasma parameters, which yields condition $r \leq 10$ that was fulfilled in the considered experiment.

If the optical thickness starts to affect the intensity of diagnostic lines under the actual experimental conditions, a diagnostic element (e.g., Al discussed in the present study) should be introduced into the target as an impurity in an amount that ensures fulfillment of the above-discussed condition of sufficient smallness of optical thickness.

Funding

This study was carried out as part of Program 10 „Experimental Laboratory Astrophysics and Geophysics at the National Center for Physics and Mathematics“ and supported by the Ministry of Science and Higher Education of the Russian Federation (state assignment № 075-00269-25-00).

Conflict of interest

The authors declare that they have no conflict of interest.

References

[1] V.V. Gavrilov, A.G. Eskov, A.M. Zhitlukhin, D.M. Kochnev, S.A. Pikuz, I.M. Poznyak, S.N. Ryazantsev, I.Yu. Skobelev, D.A. Toporkov, N.M. Umrikhin. Plasma Phys. Rep., **46** (7), 689–695 (2020). DOI: 10.1134/S1063780X20070041

[2] Y. Hirooka, N. Omoto, T. Oishi, K.A. Tanaka. Fusion Engin. Des., **87** (10), 1760–1764 (2012). DOI: 10.1016/j.fusengdes.2011.10.003

[3] Y. Hirooka, T. Oishi, H. Sato, K.A. Tanaka. Fusion Sci. Technol., **60** (2), 804–808 (2011). DOI: 10.13182/FST11-A12484

[4] C. Sánchez-Aké, D. Mustri-Trejo, T. García-Fernández, M. Villagrán-Muniz. Spectrochim. Acta B, **65** (5), 401–408 (2010). DOI: 10.1016/j.sab.2010.04.016

[5] H. Luna, K.D. Kavanagh, J.T. Costello. J. Appl. Phys., **101** (3), 033302 (2007). DOI: 10.1063/1.2431685

[6] D.S. De Young. Science, **252** (5004), 389–396 (1991). DOI: 10.1126/science.252.5004.389

[7] D.D. Ryutov, R.P. Drake, B.A. Remington. Astrophys. J. Suppl. Ser., **127** (2), 465–468 (2000). DOI: 10.1086/313320

[8] D.P. Higginson, G. Revet, B. Khiar, J. Béard, M. Blecher, M. Borghesi, K. Burdonov, S.N. Chen, E. Filippov, D. Khaghani, K. Naughton, H. Pépin, S. Pikuz, O. Portugall, C. Riconda, R. Riquier, S.N. Ryazantsev, I.Yu. Skobelev, A. Soloviev, M. Starodubtsev, T. Vinci, O. Willi, A. Ciardi, J. Fuchs. High Energy Density Phys., **23**, 48–59 (2017). DOI: 10.1016/j.hedp.2017.02.003

[9] G. Revet, S.N. Chen, R. Bonito, B. Khiar, E. Filippov, C. Argiroffi, D.P. Higginson, S. Orlando, J. Béard, M. Blecher, M. Borghesi, K. Burdonov, D. Khaghani, K. Naughton, H. Pépin, O. Portugall, R. Riquier, R. Rodriguez, S.N. Ryazantsev, I.Yu. Skobelev, A. Soloviev, O. Willi, S. Pikuz, A. Ciardi, J. Fuchs. Sci. Adv., **3** (11), e1700982 (2017). DOI: 10.1126/sciadv.1700982

[10] D.P. Higginson, B. Khiar, G. Revet, J. Béard, M. Blecher, M. Borghesi, K. Burdonov, S.N. Chen, E. Filippov, D. Khaghani, K. Naughton, H. Pépin, S. Pikuz, O. Portugall, C. Riconda, R. Riquier, R. Rodriguez, S.N. Ryazantsev, I.Yu. Skobelev, A. Soloviev, M. Starodubtsev, T. Vinci, O. Willi, A. Ciardi, J. Fuchs. Phys. Rev. Lett., **119** (25), 255002 (2017). DOI: 10.1103/PhysRevLett.119.255002

[11] C.D. Gregory, J. Howe, B. Loupias, S. Myers, M.M. Notley, Y. Sakawa, A. Oya, R. Kodama, M. Koenig, N.C. Woolsey. Astrophys. J., **676** (1), 420–426 (2008). DOI: 10.1086/527352

[12] A. Mizuta, S. Yamada, H. Takabe. Astrophys. J., **567** (1), 635–642 (2002). DOI: 10.1086/338379

[13] R. Zemskov, K. Burdonov, A. Soloviev, A. Sladkov, A. Korzhimanov, J. Fuchs, D. Bisikalo, A. Zhilkin, M. Barkov, A. Ciardi, W. Yao, M. Glyavin, M. Morozkin, M. Proyavin, A. Luchinin, P. Chuvakin, V. Ginzburg, A. Kochetkov, A. Kuzmin, A. Shaykin, I. Shaikin, S. Perevalov, A. Kotov, S. Pikuz, S. Ryazantsev, E. Khazanov, M. Starodubtsev. Astron. Astrophys., **681**, A37 (2024). DOI: 10.1051/0004-6361/202245251

[14] H.M. Al-Juboori, N.A. Malik, T. McCormack. Phys. Plasmas, **28** (12), 123515 (2021). DOI: 10.1063/5.0069277
[15] B. Albertazzi, E. Falize, A. Pelka, F. Brack, F. Kroll, R. Yurchak, E. Brambrink, P. Mabey, N. Ozaki, S. Pikuz, L. Van Box Som, J.M. Bonnet-Bidaud, J.E. Cross, E. Filippov, G. Gregori, R. Kodama, M. Mouchet, T. Morita, Y. Sakawa, R.P. Drake, C.C. Kuranz, M.J.-E. Manuel, C. Li, P. Tzeferacos, D. Lamb, U. Schramm, M. Koenig. High Power Laser Science and Engineering, **6**, e43 (2018). DOI: 10.1017/hpl.2018.37
[16] P. Mabey, B. Albertazzi, E. Falize, Th. Michel, G. Rigon, L. Van Box Som, A. Pelka, F.-E. Brack, F. Kroll, E. Filippov, G. Gregori, Y. Kuramitsu, D.Q. Lamb, C. Li, N. Ozaki, S. Pikuz, Y. Sakawa, P. Tzeferacos, M. Koenig. Sci. Rep., **9** (1), 8157 (2019). DOI: 10.1038/s41598-019-44596-3
[17] A.Y. Faenov, T.A. Pikuz, P. Mabey, B. Albertazzi, Th. Michel, G. Rigon, S.A. Pikuz, A. Buzmakov, S. Makarov, N. Ozaki, T. Matsuoka, K. Katagiri, K. Miyanishi, K. Takahashi, K.A. Tanaka, Y. Inubushi, T. Togashi, T. Yabuuchi, M. Yabashi, A. Casner, R. Kodama, M. Koenig. Sci. Rep., **8** (1), 16407 (2018). DOI: 10.1038/s41598-018-34717-9
[18] D.S. Montgomery. Rev. Sci. Instr., **94** (2), 021103 (2023). DOI: 10.1063/5.0127497
[19] N.C. Woolsey, C. Courtois, R.O. Dendy. Plasma Phys. Control Fusion, **46** (12B), B397–B405 (2004). DOI: 10.1088/0741-3335/46/12B/034
[20] J. Grava, M.A. Purvis, J. Filevich, M.C. Marconi, J.J. Rocca, J. Dunn, S.J. Moon, V.N. Shlyaptsev. Phys. Rev. E., **78** (1), 016403 (2008). DOI: 10.1103/PhysRevE.78.016403
[21] V.A. Boiko, A.V. Vinogradov, S.A. Pikuz, I.Yu. Skobelev, A.Ya. Faenov. J. Sov. Laser Res., **6** (2), 85–290 (1985).
[22] S.N. Ryazantsev, I.Yu. Skobelev, A.Ya. Faenov, T.A. Pikuz, D.P. Higginson, S.N. Chen, G. Revet, J. Béard, O. Portugall, A.A. Soloviev, A.N. Grum-Grzhimailo, J. Fuchs, S.A. Pikuz. Phys. Plasmas, **23** (12), 123301 (2016). DOI: 10.1063/1.4971805
[23] I.Yu. Skobelev, S.N. Ryazantsev, R.K. Kulikov, M. V. Sedov, S.A. Pikuz. Photonics, **10** (8), 939 (2023). DOI: 10.3390/photonics10080939
[24] A. Mignone, G. Bodo, S. Massaglia, T. Matsakos, O. Tesileanu, C. Zanni, A. Ferrari. Astrophys. J. Suppl. Ser., **170** (1), 228–242 (2007). DOI: 10.1086/513316
[25] A.Y. Faenov, S.A. Pikuz, A.I. Erko, B.A. Bryunetkin, V.M. Dyakin, G.V. Ivanenkov, A.R. Mingaleev, T.A. Pikuz, V.M. Romanova, T.A. Shelkovenko. Phys. Scr., **50** (4), 333–338 (1994). DOI: 10.1088/0031-8949/50/4/003
[26] L.A. Vainshtein, I.I. Sobel'man, E.A. Yukov. *Vozbuzhdenie atomov i ushirenie spektral'nykh linii* (Nauka, M., 1979) (in Russian).
[27] I.I. Sobel'man. *Vvedenie v teoriyu atomnykh spektrov* (Gos. Izd. Fiz.-Mat. Lit., M., 1963) (in Russian).

Translated by D.Safin